GBT MEMO 167

INITIAL PASSIVE VIBRATION MEASUREMENTS ON THE GBT

F. R. SCHWAB, J. M. PAYNE, AND D. SCHIEBEL

June 7, 1997

Abstract. We describe in this memorandum some initial measurements, using accelerometers, of the vibrations induced by random excitations of the partially completed GBT structure. For the present study, the excitation of the structure has been passive in nature: due to natural disturbances, such as wind gusts, and to construction activity. Improvements to the instrumentation which have been incorporated since the October, 1996, "shaker test" are described. Time series of measurements and derived power spectra, obtained during the first five months of 1997, are presented. Newly obtained estimates of the damping coefficient associated with the dominant modal resonance range between 0.40% and 0.48%, and are in close agreement with the results of the shaker test reported on in GBT Memo. No. 159.

1. Introduction. Previously, in GBT Memorandum No. 159, we reported the results of an experiment which was undertaken in October 1996 to investigate the dominant modal resonances of the GBT alidade structure. In this so-called "shaker test," a moving mass controlled by a hydraulic servo-mechanism was used to excite the structure, and a pair of accelerometers were used to measure the decay rate of the structural vibrations, enabling an estimate to be made of the coefficient of viscous damping associated with the dominant modal resonance. It is unlikely that we will be able to conduct any additional shaker tests during the construction phase of the GBT, because of the bulk and intrusiveness of the shaker mechanism.

However, the sensitivity of the accelerometers is such that random excitations of the structure—due, say, to wind gusts and construction activity—result in significant accelerometer output. The response of the structure to random excitations is of twofold interest: first, because such excitations are similar in nature to those which will occur when the telescope is in operation; and, secondly, because—to the extent that the power spectrum of the excitation is "white"—the power spectrum of the response should, to close approximation, be the same as that which would result from a unit-impulse excitation, since the latter type of excitation also has a white spectrum [2], [3]. We have been working, since the beginning of this year, on improvements in instrumentation and data collection, so that now it is possible at nearly all times to obtain very high-quality spectra from the time series of accelerometer data. It was necessary, in particular, to implement additional amplification, shielding, and filtering, and better analog-to-digital conversion, and to provide the means for recording substantial amounts of data.

Since January of this year we have recorded, every couple of weeks or so, one to three hours' worth of data from the accelerometers. As before, the accelerometers were mounted on the housing of one of the telescope's elevation bearings. Data were taken under varied conditions, including calm conditions of light wind and during periods of significant construction activity. The individual time series and the spectra derived from them are described in Section 2. Some data are of sufficiently high signal-to-noise ratio to obtain

estimates of the coefficients of viscous damping associated with the lowest-frequency modal resonances.

In our previous analysis of data from the shaker test, estimates of the damping coefficient were derived in two different ways: by fitting the time series of decay data via nonlinear least-squares; and by measuring the line width in the computed power spectrum. In Section 3, below, a third method—based on the Hilbert transform—is described. It yields a result which is essentially identical to that of the nonlinear least-squares analysis. This technique can also be used in passive vibration analysis. In Section 4, autocorrelation functions of the time series are presented, and the Hilbert transform is used to obtain modal parameter estimates.

From the analysis of passive vibrations, estimates of the damping coefficient associated with the dominant modal resonance range between 0.40% and 0.48%. This is in close agreement with the data from the shaker test, where the estimates ranged from 0.37% to 0.49%.

All of the data analysis, apart from the autocorrelation calculations, was done within the *Mathematica* software package.

2. Vibration Spectra from Random Excitations of the Structure. Measurements were taken on several occasions during the first five months of this year, beginning in early January. These data were obtained with the same two accelerometers as were used in the shaker test of October, 1996 (GBT Memo. 159). The instruments were mounted in the same locations—and with the same orientations—as used previously: that is, on one of the elevation-bearing housings, with the sensitive axis of the Channel 1 accelerometer aligned parallel to the elevation shaft and that of the Channel 0 accelerometer aligned perpendicular to the shaft and in the horizontal plane. The first useful data were acquired on January 10.

Time series recordings from one of the accelerometers (Ch. 1) are shown in Figure 1. Hour-long observations were taken on the first five dates, January 10 through February 19; three-hour observations on the next three dates, February 26 through March 27; and one-and-a-half-hour observations on the final three dates, April 8 through May 3. The data (not shown) from the Channel 0 accelerometer are qualitatively similar. The sampling rate was 100.16026 Hz. Data recording was done by a Model 286 PC, and the quantity of data was limited to three hours by the capacity of the floppy-disk drive. No Channel 0 data were recorded on the occasions of three hours of Channel 1 data recording. The majority of the data were taken on weekdays when workers were present on the structure and construction activity was in progress. The exceptional dates are March 15, April 13, and May 3 (a Saturday, a Sunday, and a Saturday, respectively); winds were light on the earlier two of those dates, whereas storm conditions prevailed toward the end of the May 3 observations. On days when workers were present, operation of the elevator was the cause of many of the strongest of the sporadic excitations seen in the data.

The ordinates of the time series plots show the output, in volts, from the analog-to-digital (A/D) converter, rather than actual acceleration. This is because the system gain was not well calibrated until April 8. Calibration was poor before the installation of an instrumentation amplifier, since the A/D converter had been presenting too low an impedance load to the accelerometer. On April 8 the system sensitivity was adjusted accurately to 1.0 mG/V, and on April 13 it was re-adjusted to 0.5 mG/V.

Figure 2 shows one of the time series, from April 8, in greater detail. The uppermost plot shows the entire one-and-one-half-hour span of data; the middle plot, a one-thousand-second segment of the data; and the lower plot, twenty-five seconds of data. The dominant modal resonance in the Channel 1 data of April 8 is at $\sim$1-Hz. Its signature is clearly evident in the lowermost plot, where one can count approximately twenty-five cycles.

Figures 3, 4, 5, and 6 show spectral estimates derived from each one of the time series. These estimates were computed using Welch's method of weighted and overlapped, segmented averaging of periodograms (WOSA) [4], [5]. The sampling interval of $\Delta t \approx 9.984$ ms allows the estimation of spectral components at frequencies up to $1/(2\Delta t) \approx 50$ Hz. The spectra shown in these four figures were computed using a 16,384-point sliding data window, 62.5% overlap, and a Hanning taper which was applied in the time domain. Figures 3 and 4 show the low-frequency end of the spectra—0 to 5 Hz—from the Channel 1 and Channel 0 accelerometer data, respectively. Figures 5 and 6 show the entire frequency range, from 0 to 50 Hz. Since only the data from April 8 onward were accurately calibrated, the ordinate scales of these plots, representing the power spectral densities, differ from one date to another. The first fifteen minutes of the January 29 data were omitted from the spectral computation because the telescope structure was moving in azimuth during that time.[1]

In Figure 3 we see, for the Channel 1 accelerometer, the dominant modal resonance frequency starting out at ~1.25 Hz on January 10 and remaining near that value until February 26. By March 15 it has shifted down to ~1 Hz, and between April 8 and April 13 it has shifted back up to ~1.25 Hz. The second-lowest-frequency modal resonance wanders considerably and is typically near 1.8 Hz. David Parker kindly furnished us with the following chronology of construction activity:

- *January 8, 1997:* The left feed-arm modules C and D are in place;
- *February 3, 1997:* Actuator room is in place;
- *February 25, 1997:* Right feed-arm modules C and D are in place;
- *April 11, 1997:* The tipping structure is moved from 77° elevation to 66° elevation;
- *April 29, 1997:* Feed-arm section F is in place.

It seems likely that the cause of the upward shift in the dominant resonance was the elevation change on April 11. (The cause of the earlier downward shift might have been the completion of installation and welding of the right feed-arm C and D modules, combined with removal of crane support—but this inference is somewhat speculative.)

In Figure 4, for the Channel 0 accelerometer data, we see the dominant modal resonance typically at ~1.8–1.9 Hz. Frequently a line appears at the same frequency as the Channel 1 dominant resonance. We have not determined whether this is a spurious response due to misalignment of the accelerometer. Also, the Channel 0 spectra show significant evidence of aliased high-frequency electrical interference, especially the data from January 29 and February 19. Figure 6 shows strong spectral energy at the higher frequencies, typically including some clutter around ~20 Hz and ~42–46 Hz.

Analog lowpass filtering—with a cutoff frequency at 20 Hz—was applied to all of the data, for anti-aliasing. A very-sharp-cutoff active filter was installed on March 27 because interference problems had become apparent. In Figures 5 and 6 the sharper response of this filter is clearly evident. This is a six-pole Chebyshev filter with 0.5 dB maximum passband ripple. Its phase characteristics are probably not good enough for possible future applications, such as time-domain mode tracking. Welding was occurring during the time of many of our observations; this probably accounts for much of the interference. Figure 7 shows an interesting set of data from a three-hour period on February 26, when very major construction activity was taking place. The apparent splitting of the dominant resonance line in this plot is probably due to aliased high-frequency interference.

Figure 8 shows spectra from another three hours of data taken on March 27, just after installation of the active filter. The improvement in data quality is apparent; moreover, the

[1] Those data may, in fact, be of interest in their own right.

noise in the computed spectra averages down much better than in the earlier observations. Typically our spectra show about 50 dB dynamic range. The noise floor, which in Figure 8 is at about -80 dB, is due, we believe, to quantization noise from the 16-bit A/D conversion.

Excellent-quality data were obtained again on April 8 and 13. High-resolution (Ch. 1) spectral estimates derived from these data are shown in Figures 9 and 10. These spectra were computed via the WOSA method with a 32,768-point data window, uniform weighting, and 50% overlap. Here the signal-to-noise ratio is sufficient to obtain reasonable estimates of the full-width at half-maximum of the dominant resonance. The corresponding estimates of the viscous damping ratio associated with the dominant resonance are $\zeta \approx 0.0040$ (or 0.40%) and $\zeta \approx 0.0048$ (or 0.48%) for the two dates—which is in reasonable agreement with our results from the shaker test (Memo. 159).

Finally, the *Mathematica* software developed during the course of our work can also be used for the computation of cross-spectra. An example is shown in Figure 11. Cross-spectral estimates based on data from multiple sensors will likely be essential for the identification and characterization of structural vibration modes.

It would have been interesting to compare the computed spectra with predictions from finite-element modeling, but this was not possible because the only modeling that has been done (or which is planned) is modeling of the complete telescope design. It would be somewhat impractical to model the telescope at very many phases of completion, because of the computational expense and the manpower requirements. Also, whenever large substructures happen to be hinged into place but not completely welded—and perhaps partially supported by crane lines—the observed spectra appear to be significantly altered, and therefore any detailed analysis is easily confounded by practical realities.

3. Re-Analysis of Data from the Shaker Test. In the so-called "shaker test" which we reported on in GBT Memorandum No. 159, a moving mass controlled by a hydraulic servo-mechanism was put into sinusoidal motion and used to excite the dominant modal resonance of the structure. The Channel 1 accelerometer was used to observe the decay of the vibrations. Estimates of the viscous damping coefficient associated with the dominant resonance were derived in two different ways: by fitting the time series of decay data via nonlinear least-squares; and by measuring the line width in the computed power spectrum. The time-domain method (in this case, nonlinear least-squares) is expected to have yielded a more accurate estimate of the damping coefficient. This is because any frequency-domain spectral width estimate is artificially broadened because of the finite duration of the time series (in the present case, 100 seconds).

After Memo. 159 was written, the thought occurred to one of us that a different time-domain method could have been used: namely, one based on the (discrete) Hilbert transform. The Hilbert transform $f^{\natural}$ of a function $f(t)$ can be defined either via the principal value integral

$$f^{\natural}(t) = -\frac{1}{\pi} \int_{-\infty}^{\infty} \frac{f(t')}{t - t'} \, dt' \,,$$

or, via the Fourier transform, according to the formula $f^{\natural}(t) = [f^{\wedge}(\gamma)\,\mathrm{sign}(\gamma)]^{\vee}(t)$, where $^{\wedge}$ denotes Fourier transformation and $^{\vee}$ denotes inverse Fourier transformation (see, e.g., [6], [7]). The discrete Hilbert transform is defined analogously, via the Fourier transform formula, in terms of the discrete Fourier transform. The instantaneous envelope of a real-valued signal $f(t)$ is given in terms of the Hilbert transform by $\sqrt{f(t)^2 + f^{\natural}(t)^2}$, and the instantaneous frequency is given by the derivative of the instantaneous phase, $\arctan \frac{f^{\natural}(t)}{f(t)}$, of the so-called "analytic signal," $f(t) + i f^{\natural}(t)$.

The envelope of the time series of decay data from the shaker test, computed via the discrete Hilbert transform, is shown, on a semi-log scale, in Figure 12. A straight line was fit to the computed envelope via linear least-squares. The best-fitting slope of -0.0286 yields an estimate of $\zeta = 0.00370$ for the viscous damping ratio. This agrees to within about one-percent with the value ($\zeta = 0.00374$) that was derived by nonlinear least-squares in Memo. 159. The Hilbert transform method is much simpler and much less computationally expensive (by at least a factor of 100, or so) than the nonlinear least-squares approach. The use of Hilbert transform techniques in the context of structural vibration analysis is also discussed in [8] and references cited therein.

4. Correlation Analysis of Passive Vibration Measurements. Plots of the computed autocorrelations of the accelerometer time series provide a very direct portrayal of the decay rates of the dominant modes—more so, we believe, than do plots of the line shapes in the spectra (see Fig. 13). (In [3], [9], it is shown that the autocorrelation of the response of a lightly damped system to white-spectrum random excitation decays at the same rate as the impulse response of the system.) Figure 13 shows autocorrelation functions $r(\tau)$ computed from the $1\frac{1}{2}$-hour time series of accelerometer data of April 8 and April 13, plotted for time lags τ between 0 and 500 seconds. Noise in the response—for example, sensor noise, amplifier noise, and A/D quantization noise—causes a spike which is concentrated near the zero lag, $\tau = 0$, [3]. Since the Channel 0 data are significantly noisier than the Channel 1 data, the spikes have been suppressed in the Channel 0 plots in order to allow an enlarged view of the more interesting part of the data. Relatively stronger damping is apparent in the Channel 0 data than in the Channel 1 data. An expanded view of the Channel 0 data, for τ between 0 and 100 seconds, is shown in Figure 14, where the absence of a single dominant mode is evidenced by the strong modulation of the envelope of the autocorrelation.

In the case of the Channel 1 data, which are dominated by a single modal resonance, the Hilbert transform can be used to compute the envelope of the autocorrelation, and the damping coefficient then can be estimated by fitting to the data from the initial time lags, say $|\tau| < 50$ or 80 seconds. The autocorrelation function computed from the Channel 1 data of April 13 is shown in Figure 15, together with the computed envelope and the best-fitting exponential-decay curve. The estimated damping coefficient is $\zeta = 0.0042$ (or 0.42%) for the 1.25-Hz modal resonance. The fit to the data from April 8—which is shown in Figure 16—is not quite as good. Here the estimate of damping is $\zeta = 0.0047$ (or 0.47%). We have not quoted error bars because the formal error estimates appear to be unrealistically small.

It would be possible to extend this type of analysis. The Hilbert transform method can be used to obtain damping estimates for higher-order modes, if notch filters are first applied to the time series [8]. Alternatively, various algebraic decomposition methods can be used in correlation analysis; such an approach was taken in a study of one of the JPL Deep Space Network tracking antennas [10].

In this part of our work, we used a direct computation—via a Fortran program—of the autocorrelation functions, and equal numbers of lagged products were taken in each summation. There was no tapering of the autocorrelations, either direct or (as would have occurred if the WOSA method had been used) indirect.

5. Plans for Future Work. To date, the accelerometer data acquisition has been handled by a dedicated PC. Within the next few months it should be possible to integrate this task within the GBT Monitor and Control System. For the recent data we have used 16-bit A/D conversion and a 100-Hz sampling rate. This results in relatively large volumes of data, and we will need to investigate what limitations there may be in the ability to record and archive this type of data within the Monitor and Control System.

Don Wells, in GBT Memorandum No. 161, advocates equipping the GBT with multiple accelerometers and discusses the possibility of using less expensive units than the inertial-navigation-grade Allied Signal QA-2000's which we have used to date. Allied Signal has recently introduced an accelerometer designed for industrial applications: the QLC-400, with technical specifications approaching those of the QA-2000, but only one-fifth as expensive. We have purchased a few of these units, and plan to test them thoroughly. In the case of multiple accelerometers, the data sampling should be synchronous (simultaneous sample-and-hold) to eliminate systematic biases in estimates of the phases of the signals [12].

There has been some discussion (e.g., in Memo. 161) of building an active-mass-driven damping system to control the feed-arm oscillations. The control algorithm for such a system would likely employ acceleration feedback. If higher-order modes need to be tracked and controlled, then stringent requirements may be imposed upon the instrumentation associated with the accelerometers. In particular, the programmable antialising filters which are used by the Notre Dame group who work in aseismic protection are described as follows [12]: "The XFM82 series filters offer programmable pre-filter gains to amplify the signal into the filter, programmable post-filter gains to adjust the signal so that it falls in the correct range for the A/D converter, and analog antialiasing filters which are programmable to 25 Hz. The high-quality elliptic low-pass filter has a 0.001 dB pass-band ripple, a stop-band magnitude of -90 dB, and a 90 dB/oct roll-off above the cutoff frequency. The filters on all 8 channels are magnitude/phase matched to within 0.1 dB/1 degree to 90% of the cutoff frequency." This amounts to considerably more sophisticated signal conditioning than we have implemented. We plan to establish contact with other researchers, in order to benefit from their experiences.

Bandwidth, command-and-control, and signal-conditioning requirements, in general, for various uses of the accelerometer data need to be established.

Once the construction of the GBT is completed, we will want to study very carefully and intensively the spectra of the structural vibrations and compare them with finite-element model predictions.

References

[1] J. M. Payne, D. Schiebel, and F. R. Schwab, "Dynamic Tests on the GBT", GBT Memo. No. 159, October 24, 1996.

[2] B. L. Clarkson and C. A. Mercer, "Use of cross correlation in studying the response of lightly damped structures to random forces", *AIAA J.*, **3** (1965) 2287–2291.

[3] F. Kandianis, "Frequency response of structures and the effect of noise on its estimates from the transient response", *J. Sound Vib.*, **15** (1971) 203–215.

[4] P. D. Welch, "The use of fast Fourier transform for the estimation of power spectra: a method based on time averaging over short, modified periodograms", *IEEE Trans. Audio & Electroacoust.*, **AU-15** (1967) 70–73.

[5] D. B. Percival and A. T. Walden, *Spectral Analysis for Physical Applications: Multitaper and Conventional Univariate Techniques*, Cambridge Univ. Pr., Cambridge, 1993.

[6] H. Dym and H. P. McKean, *Fourier Series and Integrals*, Academic Pr., 1972, p. 93.

[7] R. H. Bracewell, *The Fourier Transform and its Applications*, Second Ed., McGraw–Hill, 1978, pp. 267 ff.

[8] A. Agneni, "Modal parameter estimates from autocorrelation functions of highly noisy impulse responses", *Int. J. Analytical & Experimental Modal Analysis*, **7** (1992) 285–297.

[9] F. Kandianis, "Correlation techniques in the analysis of transient processes", *J. Sound Vib.*, **26** (1973) 161–172.

[10] *Dynamic Testing and Correlation of the DSS-24 34 Meter Beam Waveguide Antenna*, Engineering Report issued under Defiance–STS/SMC Project No. 63257 and JPL Contract No. 960129.

[11] D. C. Wells, "Approaches to the GBT Vibration Problem", GBT Memo. No. 161, December, 1996.

[12] S. J. Dyke, B. F. Spencer, Jr., P. Quast, D. C. Kaspari, Jr., and M. K. Sain, "Implementation of an AMD using acceleration feedback control", *Microcomputers in Civil Engineering: Special Issue on Active and Hybrid Structural Control*, to appear.

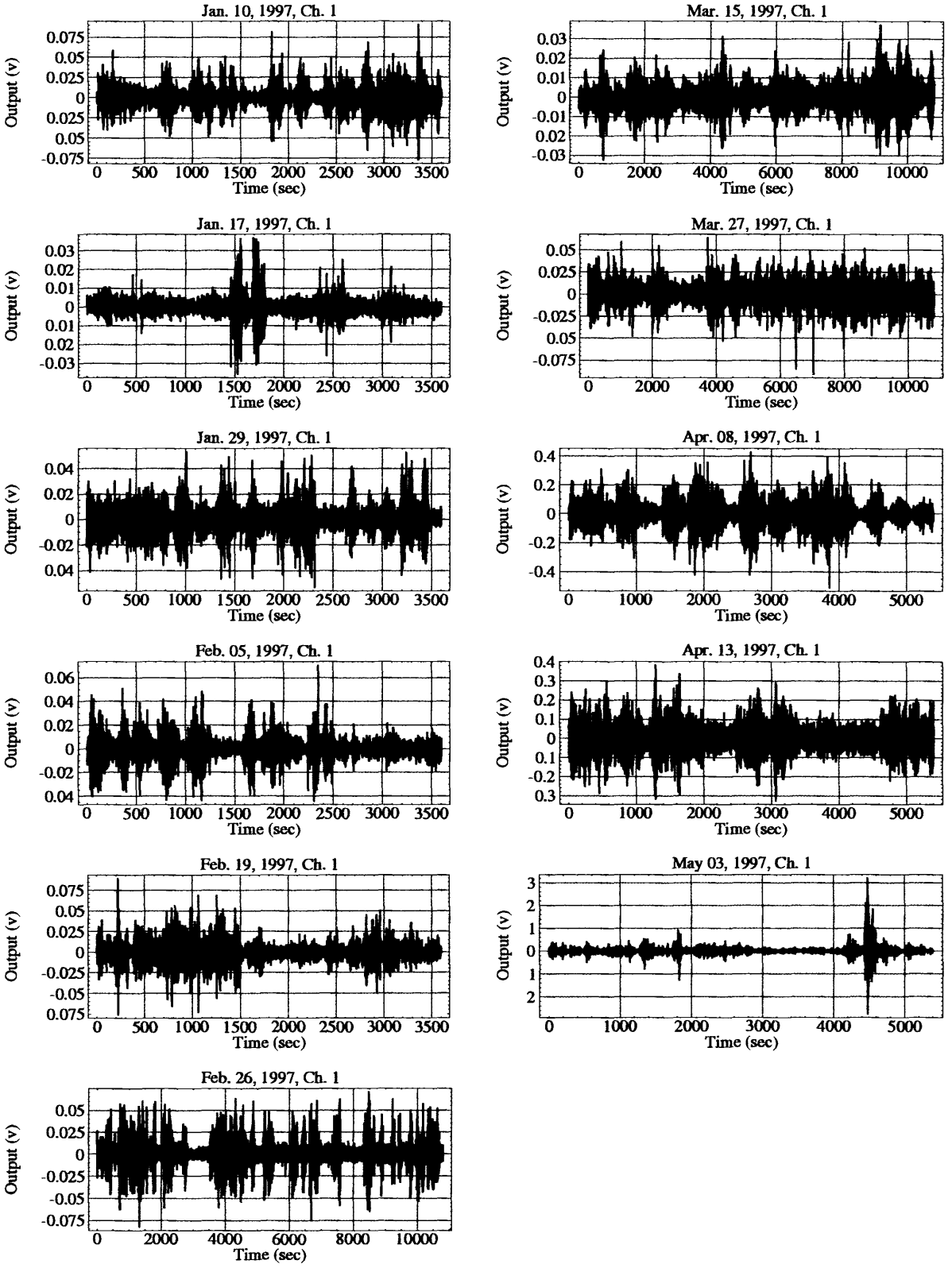

Figure 1. Time series records from the Channel 1 accelerometer obtained during the first five months of 1997. Because the system gain was not well calibrated before the installation of instrumentation amplifiers on April 8, the ordinates are labeled with the output voltage from the analog-to-digital converter rather than in units of acceleration. On April 8 the system sensitivity was adjusted accurately to 1 mG/V, and on April 13 it was re-adjusted to 0.5 mG/V.

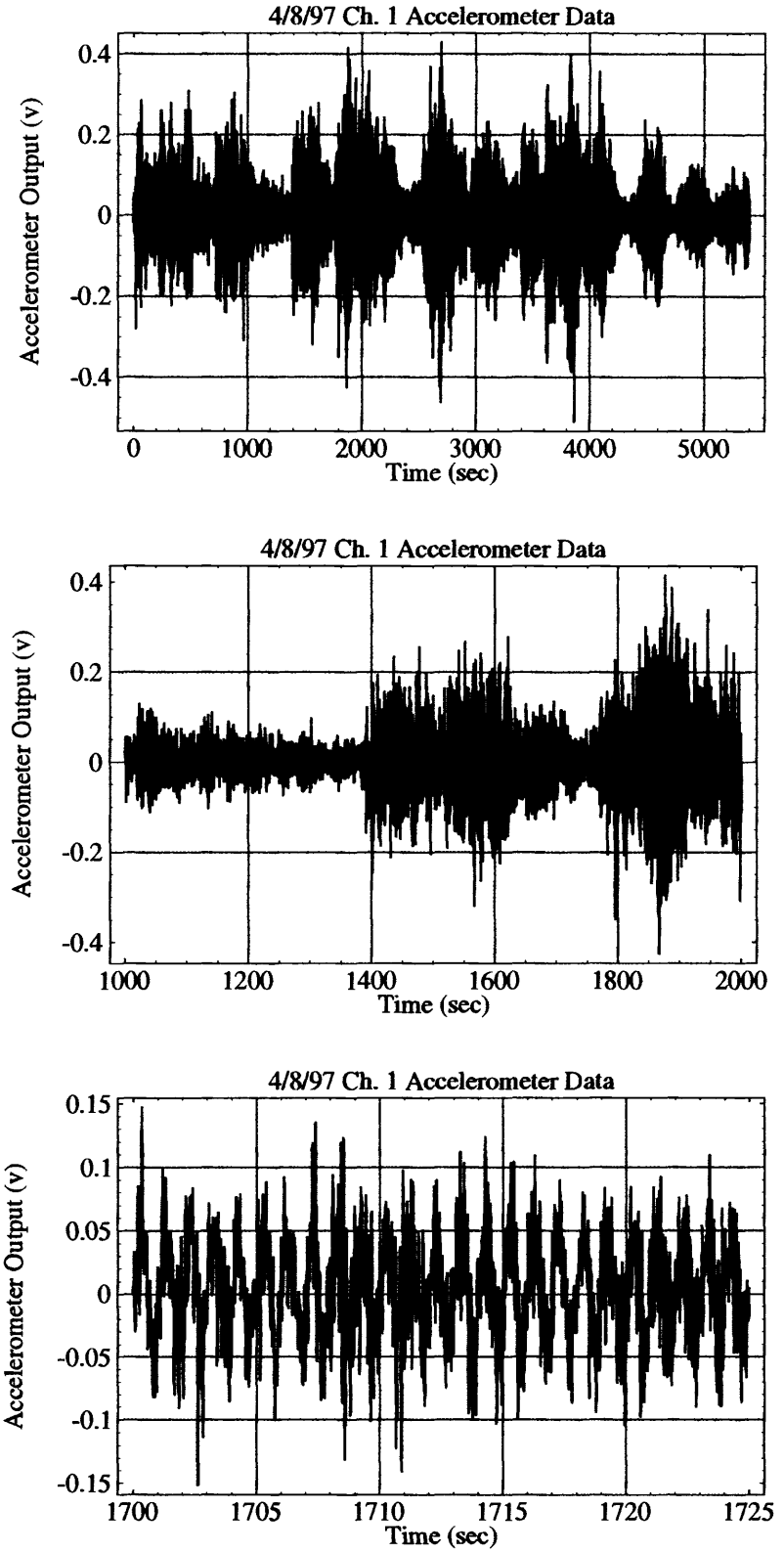

Figure 2. A $1\frac{1}{2}$-hour time series recorded by the Channel 1 accelerometer on April 8, 1997. *(Top)* The entire recording. *(Middle)* A 1000-second segment of the recording. *(Bottom)* A twenty-five second segment; here the $\sim$ 1-Hz modal resonance is evident.

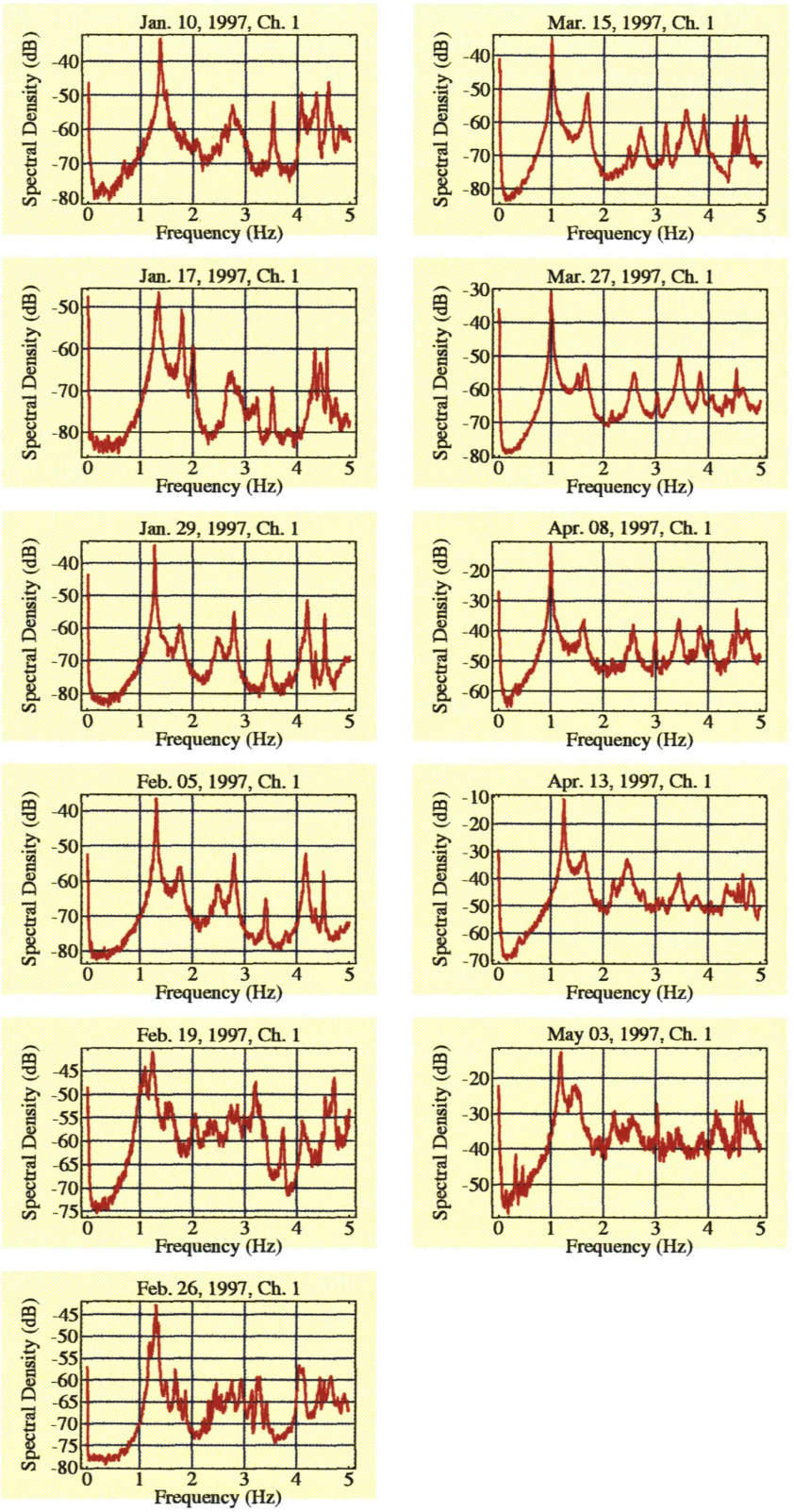

Figure 3. Spectral estimates from the Channel 1 accelerometer, mounted parallel to the elevation shaft, plotted over the range 0–5 Hz.

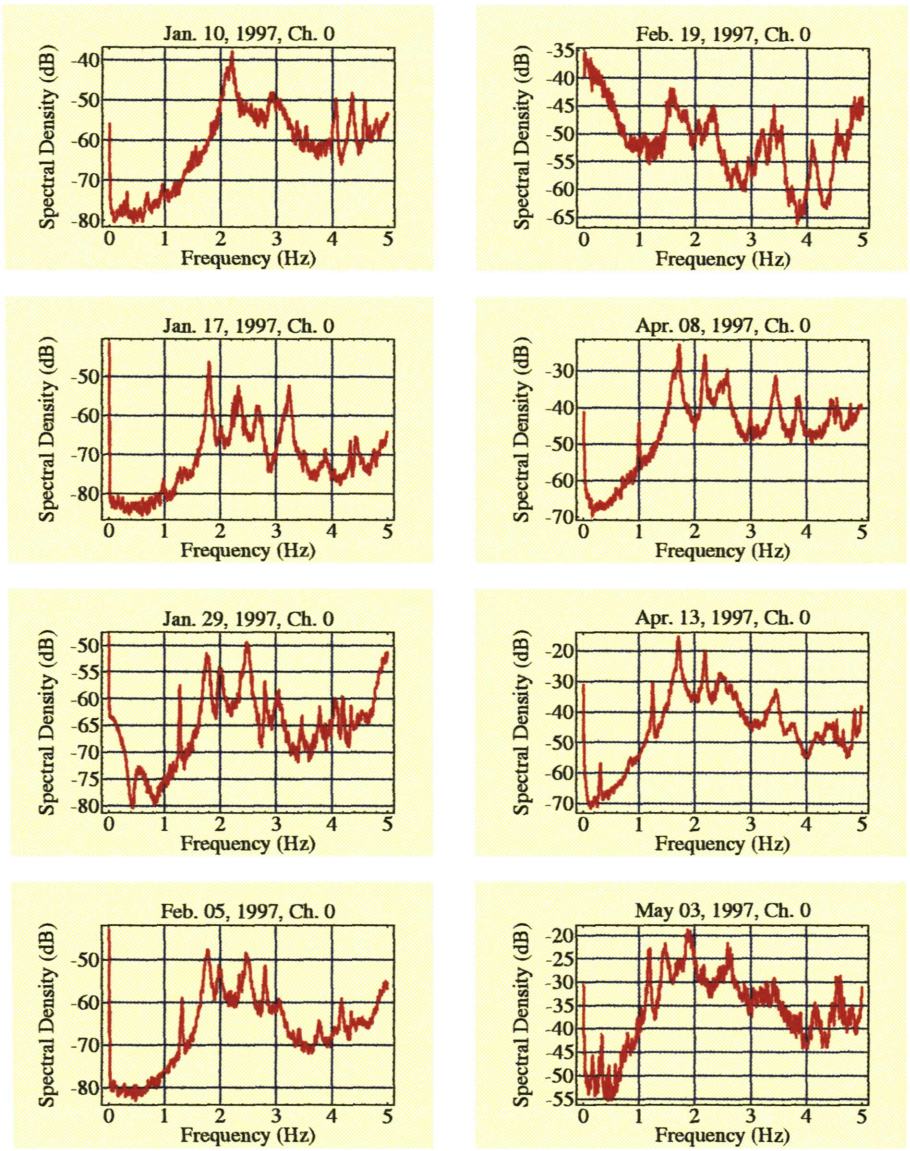

Figure 4. Spectral estimates from the Channel 0 accelerometer, mounted perpendicular to the elevation shaft, plotted over the range 0–5 Hz. The spectra for January 29 and February 19 appear to be severely corrupted by aliased high-frequency interference (cf. Fig. 6).

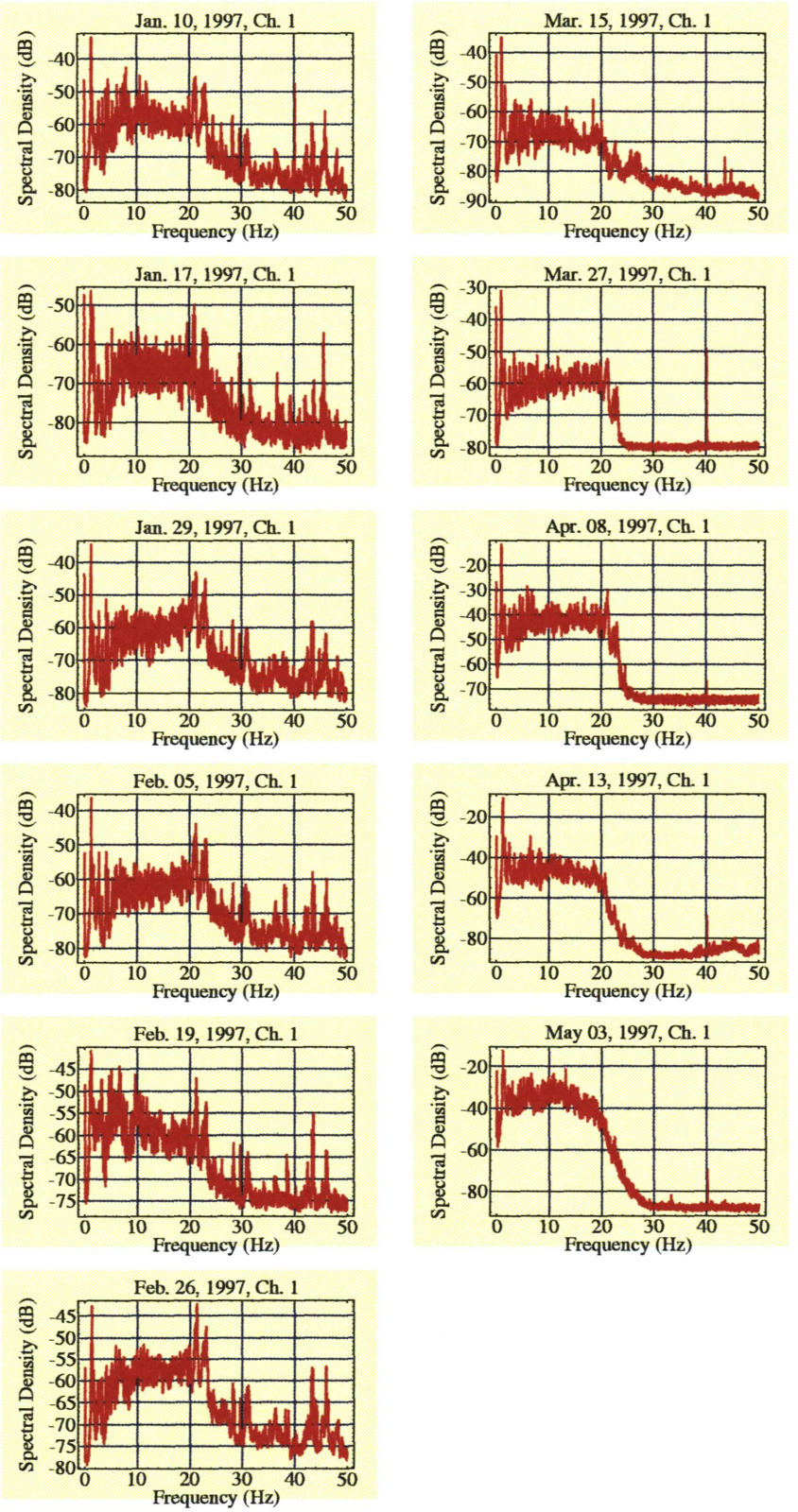

Figure 5. Spectral estimates from the Channel 1 accelerometer, mounted parallel to the elevation shaft, plotted over the range 0–50 Hz. The active filter was used for data taken from March 27 onward. In the spectra taken after that data, the evidence of 60-Hz power-line noise (which aliases in at 40 Hz) is still quite apparent.

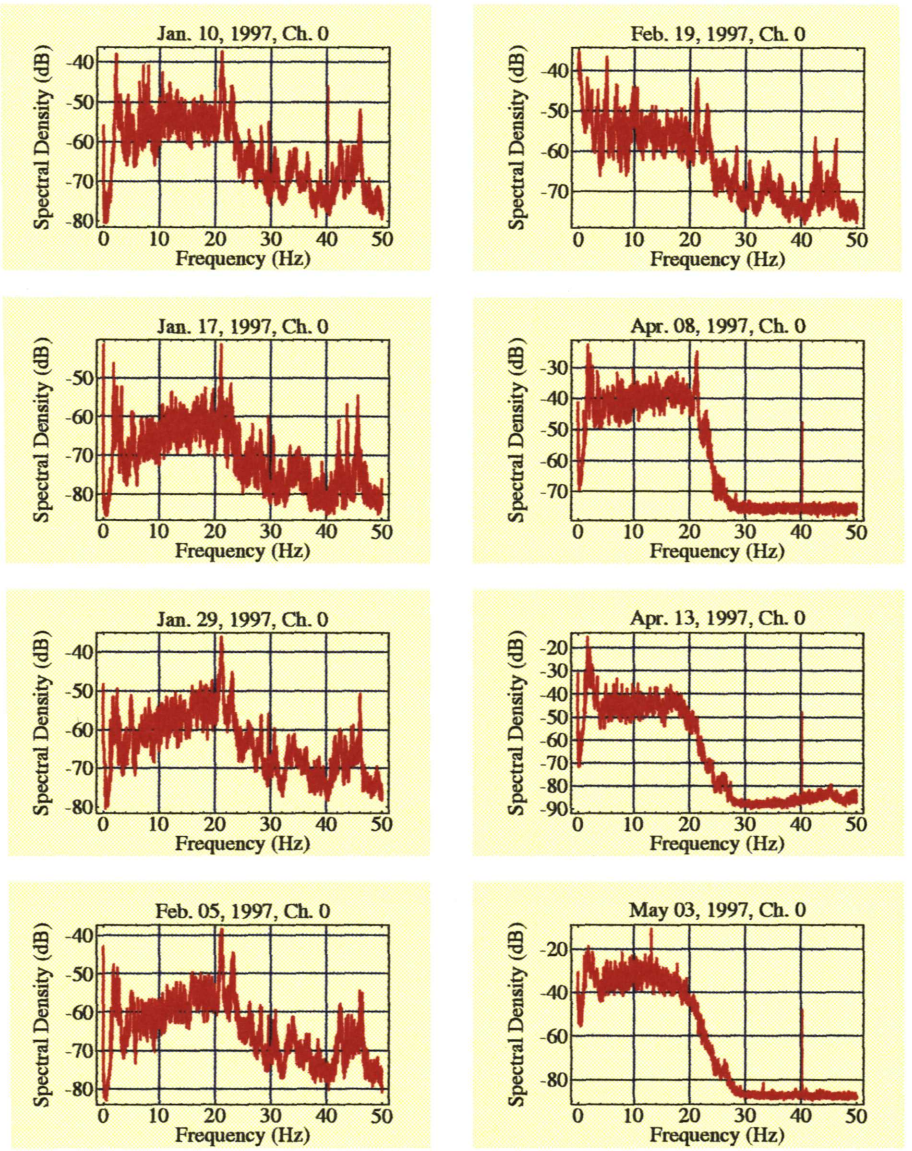

Figure 6. Spectral estimates from the Channel 0 accelerometer, mounted perpendicular to the elevation shaft, plotted over the range 0–50 Hz. The clutter around ~20 Hz, which sometimes dominates the Channel 0 spectra, is of unknown origin and may be an alias of higher frequency electrical interference.

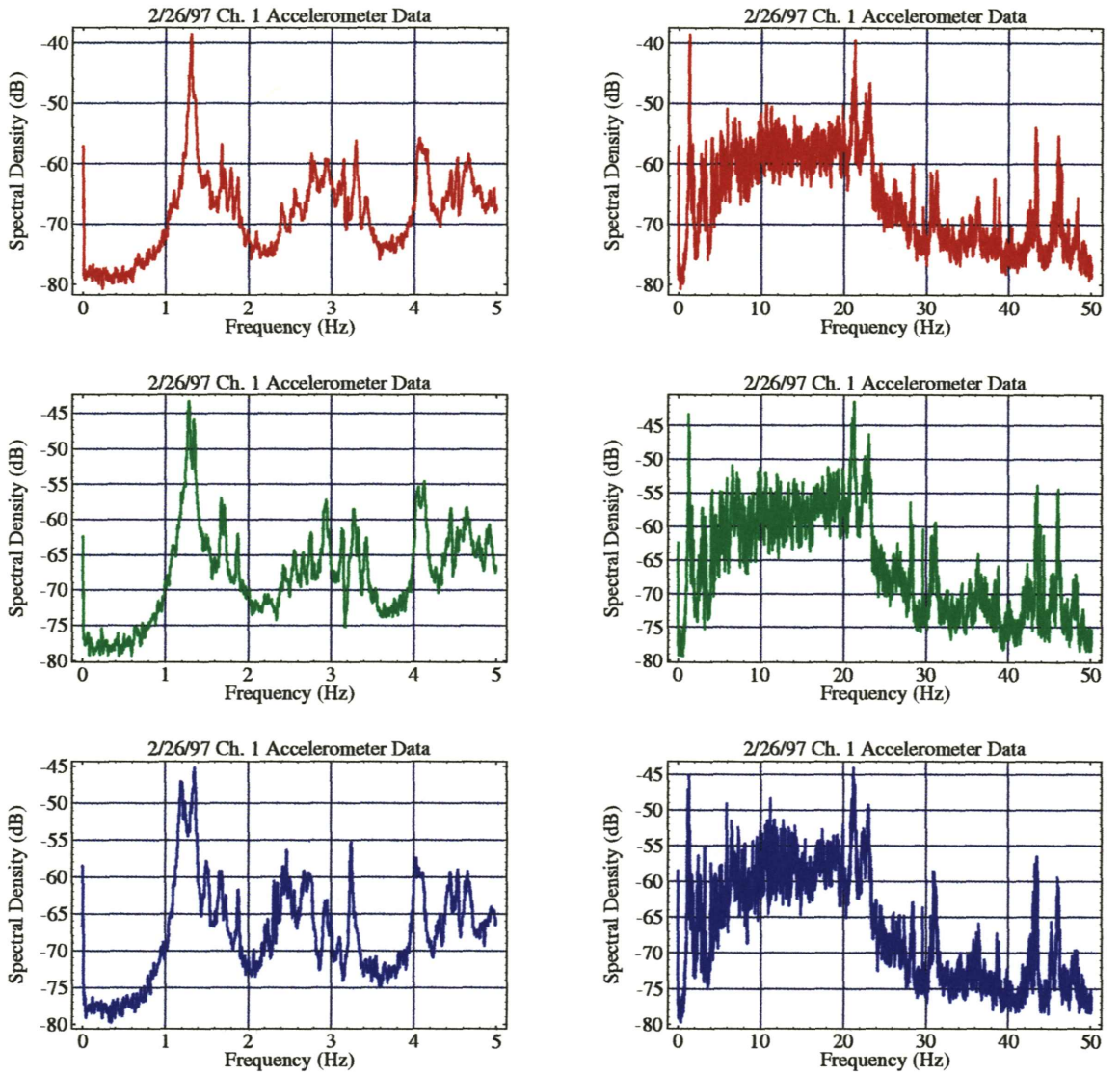

Figure 7. Spectra for three consecutive one-hour periods, obtained with the Channel 1 accelerometer on February 26, 1997, while construction was in progress and as a very large structural member was being attached to the horizontal feed-arm assembly. These data were obtained before installation of the active filter; many of the spectral features are extraneous and due to aliased high-frequency interference. The apparent splitting of the dominant modal resonance probably is not real.

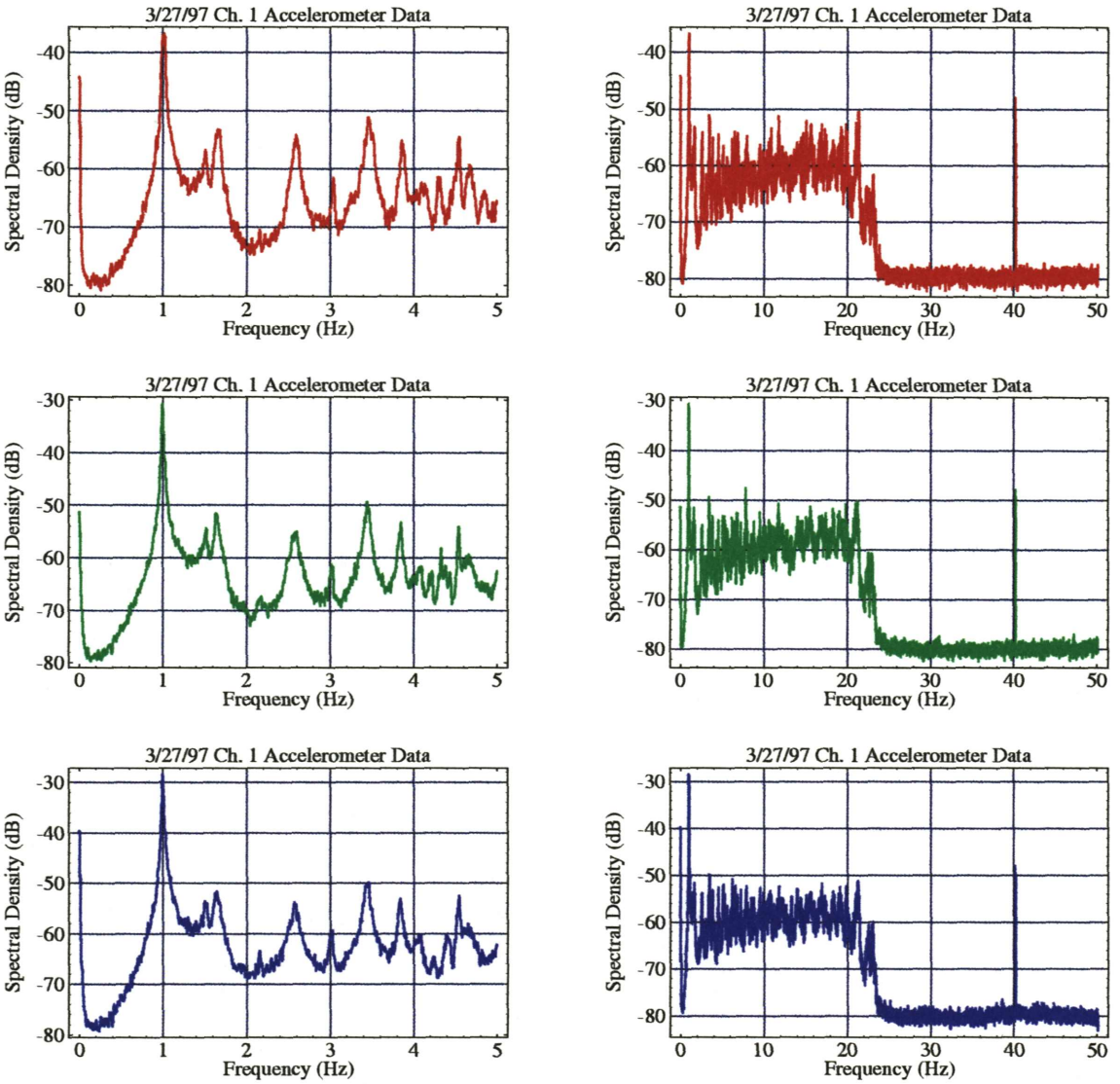

Figure 8. Spectra for three consecutive one-hour periods, obtained with the Channel 1 accelerometer on a weekday under conditions of light winds, when some construction activity was occurring. These data were taken on March 27, just after installation of the active filter.

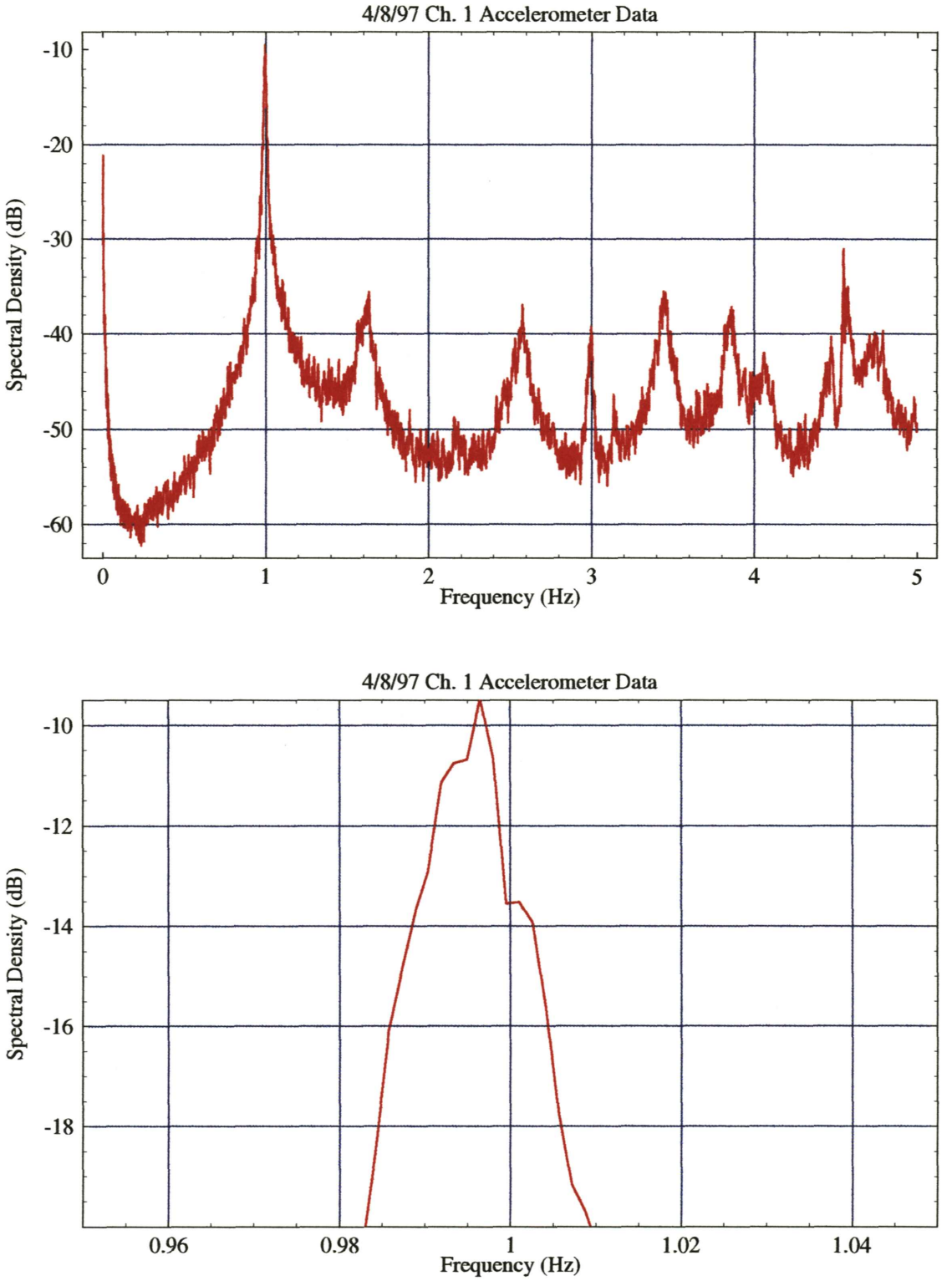

Figure 9. *(Top)* Spectral estimate derived from the April 8, 1997, Channel 1 accelerometer data, plotted over the range 0–5 Hz. The dominant modal resonance is at ~1 Hz. This spectrum was computed from 90 minutes of data using a 32,768-point sliding data window, 50% overlap, and no tapering. *(Bottom)* Detailed view of the 1-Hz modal resonance line. The 3-dB width of ~0.008 Hz yields an estimate of $\zeta \approx 0.004$ (or 0.4%) for the viscous damping ratio.

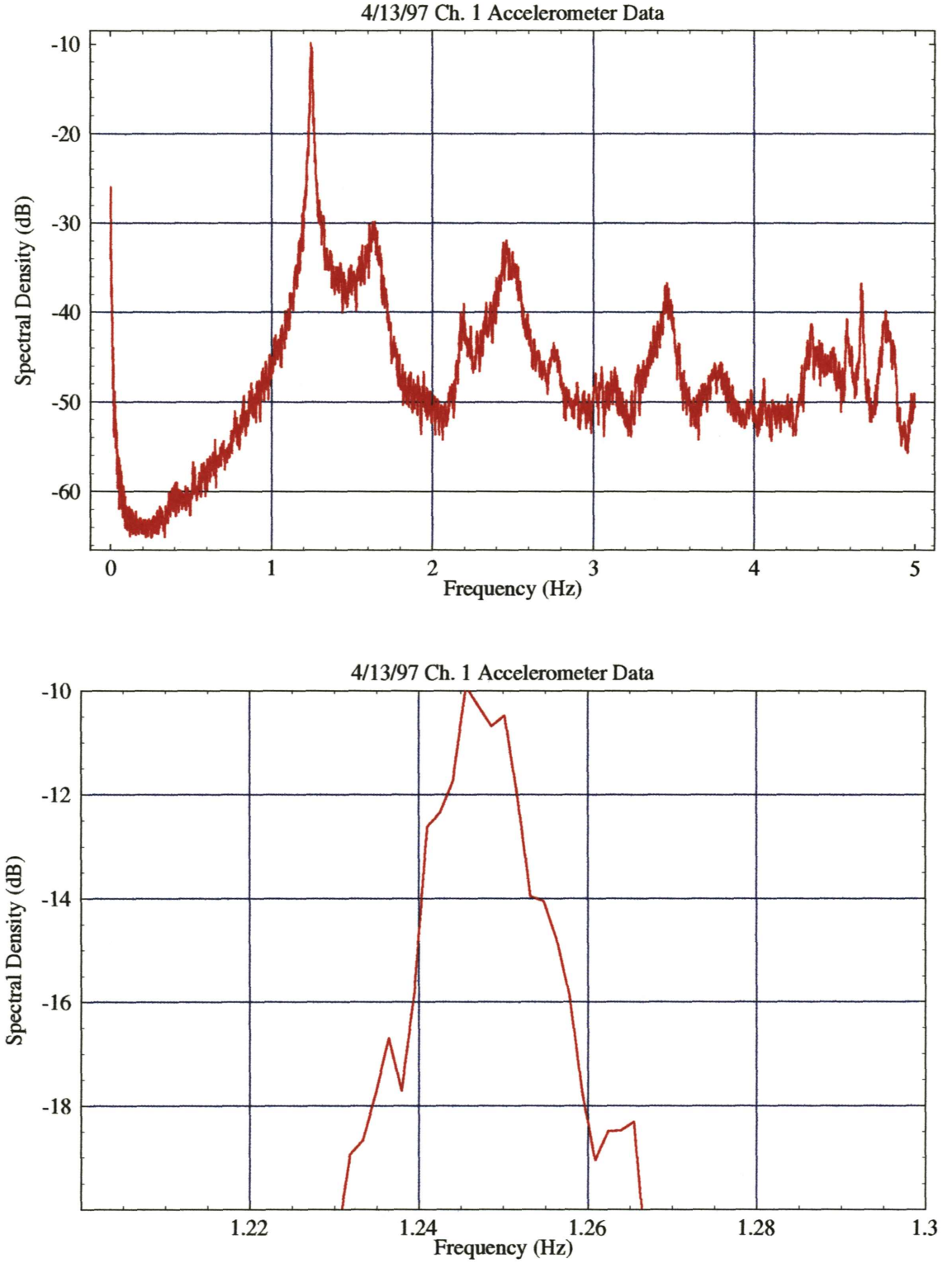

Figure 10. *(Top)* Spectral estimate derived from the April 13, 1997, Channel 1 accelerometer data, plotted over the range 0–5 Hz. The dominant modal resonance is at ~1.25 Hz. This spectrum was computed from 90 minutes of data using a 32,768-point sliding data window, 50% overlap, and no tapering. *(Bottom)* Detailed view of the 1.25-Hz modal resonance line. The 3-dB width of ~0.012 Hz yields an estimate of $\zeta \approx 0.0048$ (or 0.48%) for the viscous damping ratio. The shift in the resonance line from ~1 Hz to ~1.25 Hz (since April 8) is likely due to the fact that the tipping structure was moved from 77° elevation to 65° on April 11.

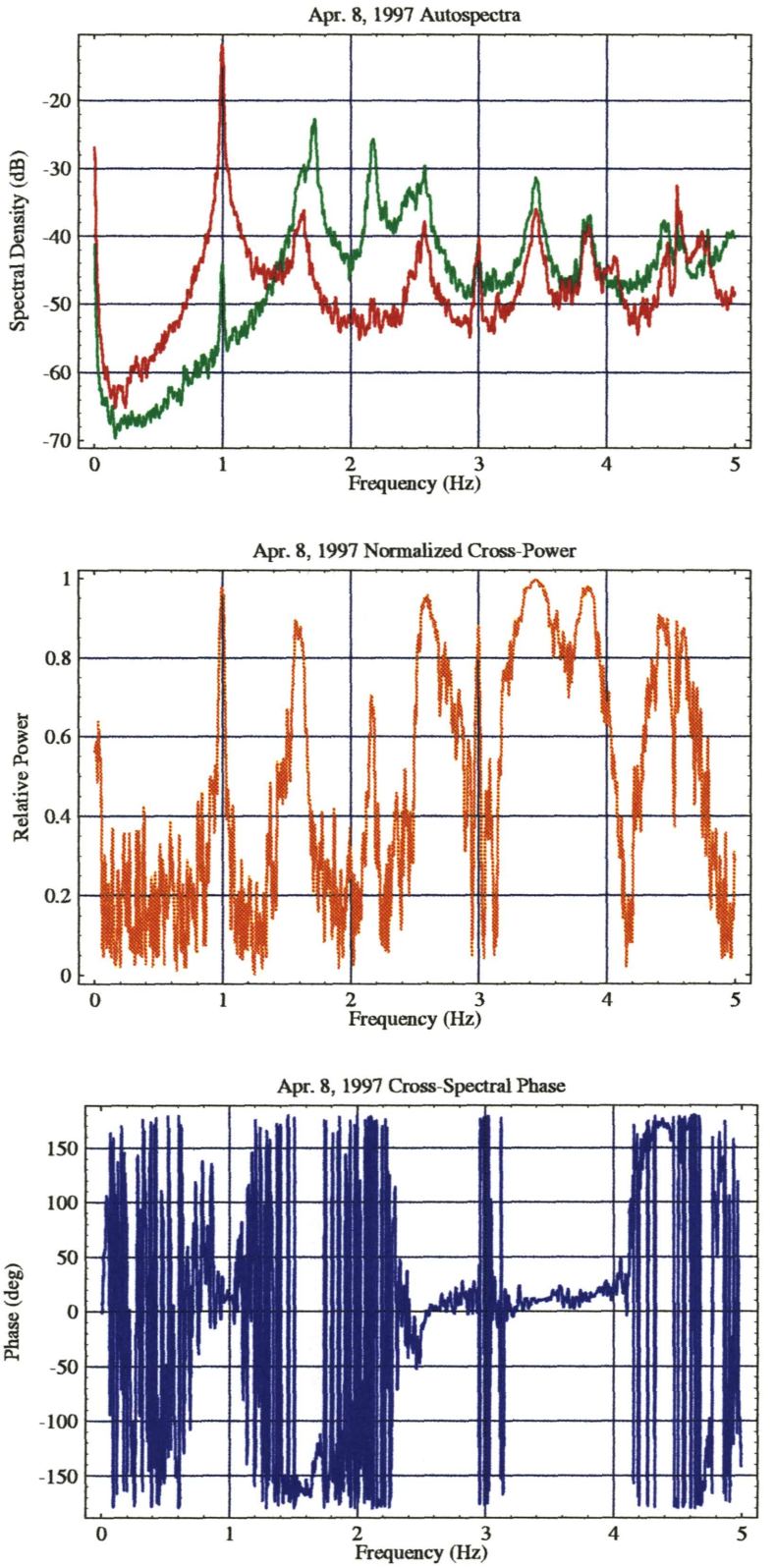

Figure 11. A sample cross-spectral estimate, derived from the April 8, 1997, data. *(Top)* The Channel 0 and Channel 1 autospectra are plotted in green and red, respectively; *(Middle)* The normalized cross-power spectrum, plotted on a linear scale, shown in orange; *(Bottom)* The cross-spectral phase, displayed in blue.

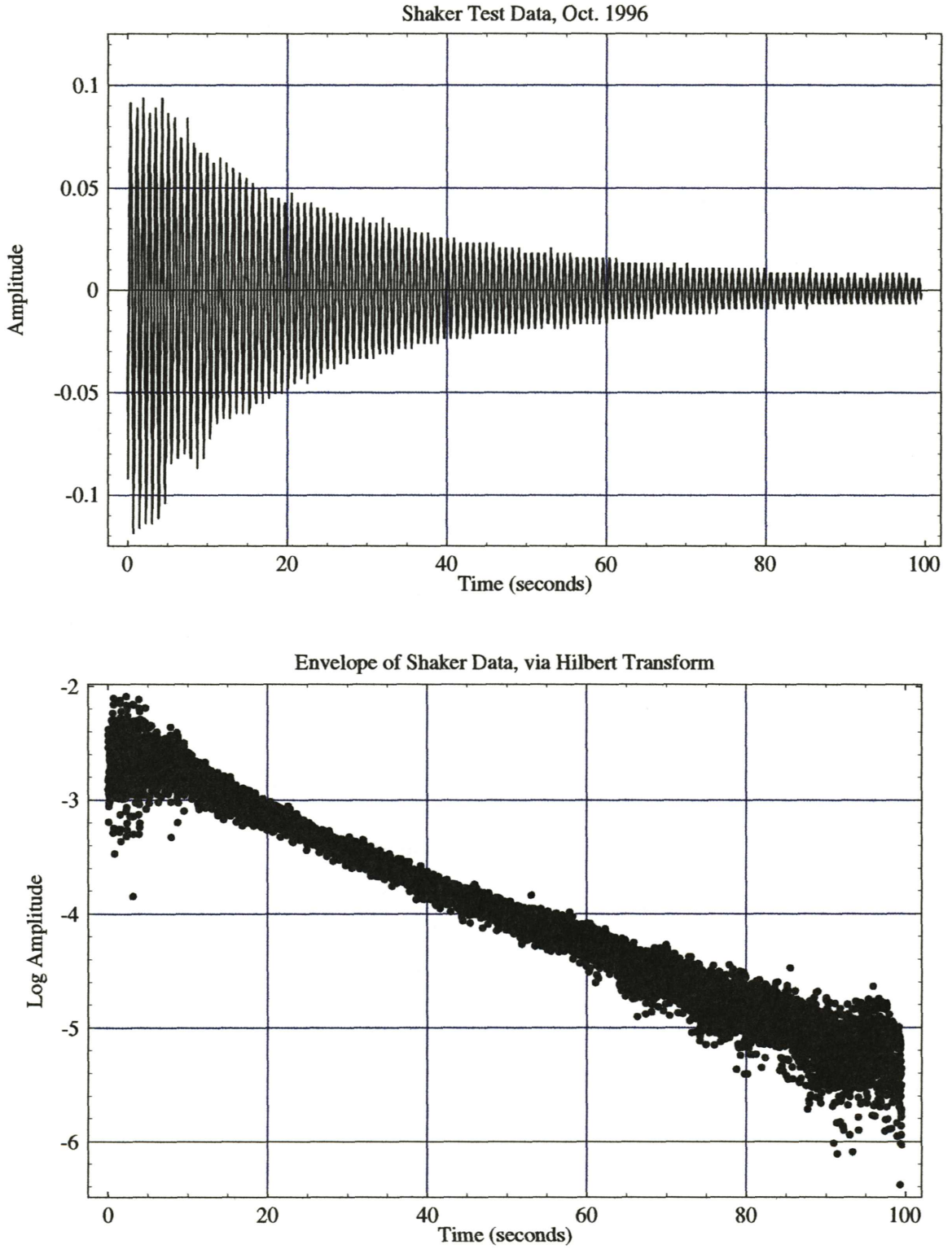

Figure 12. *(Top)* The "shaker" data from October, 1996. *(Bottom)* Envelope of the shaker data computed via the Hilbert transform, shown on a logarithmic scale. (The natural logarithm is used.) The best-fit slope of -0.0286 yields an estimate of $\zeta = 0.00370$ for the viscous damping coefficient associated with the dominant modal resonance, which was at 1.23-Hz on the date of the shaker test.

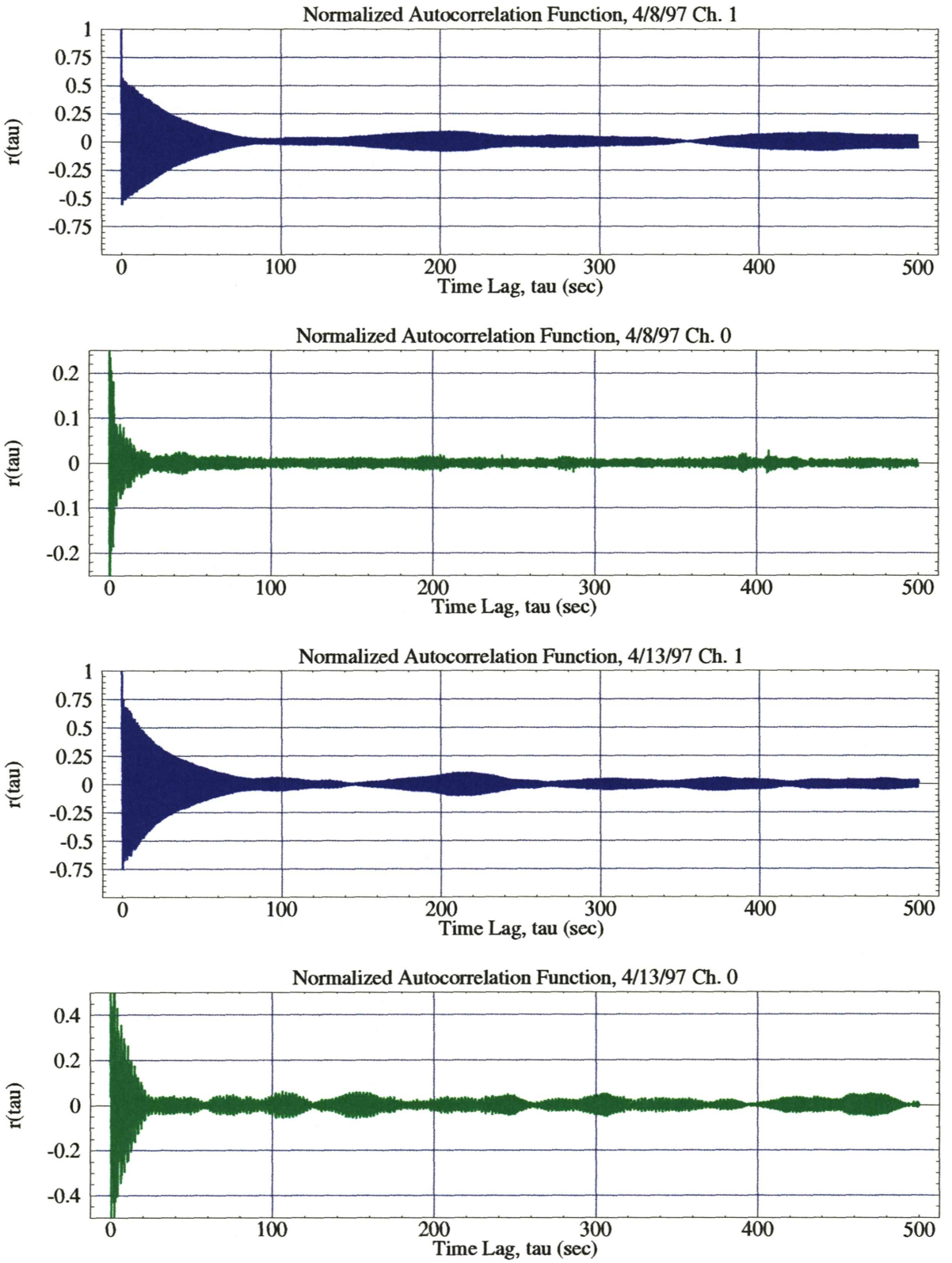

Figure 13. Autocorrelation functions computed from the time series of accelerometer data of April 8 and April 13, 1997, for time lags τ between 0 and 500 seconds.

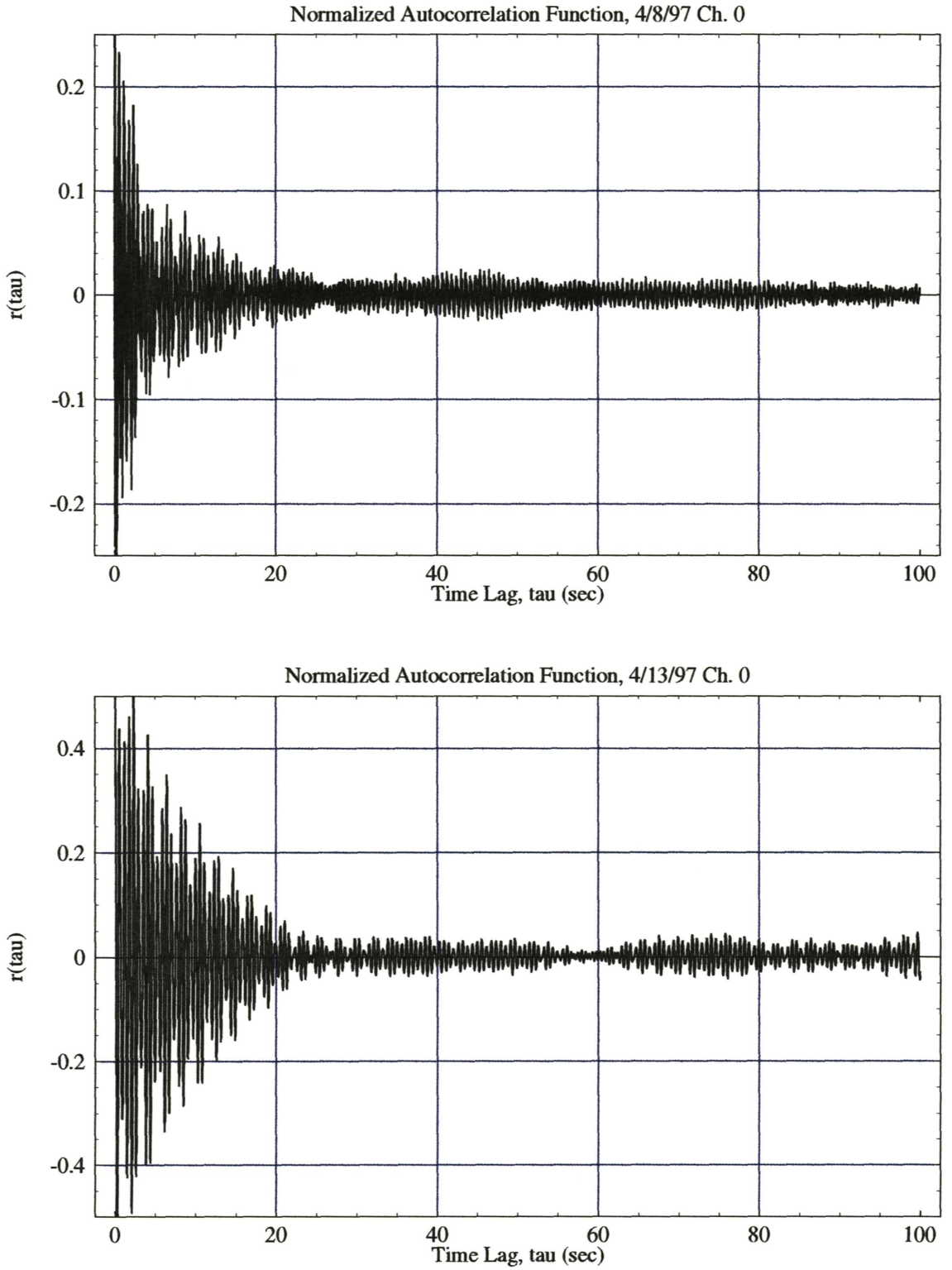

Figure 14. Autocorrelation functions computed from the time series of Channel 0 accelerometer data of April 8 and April 13, 1997, for time lags τ between 0 and 100 seconds. Relatively stronger damping is apparent, compared with the Channel 1 data. The absence of a single dominant modal resonance is evidenced by the strong modulation of the envelope of the autocorrelation.

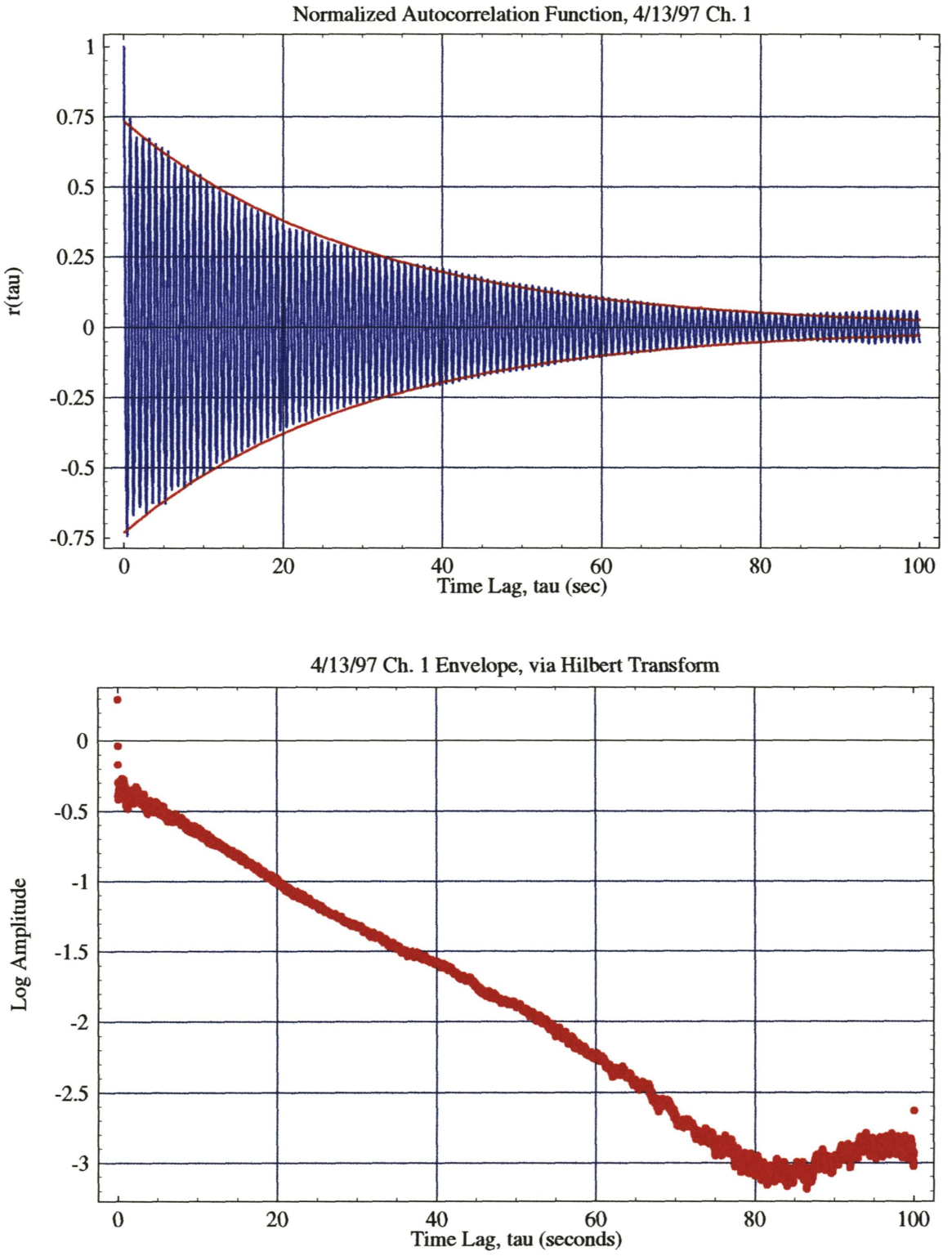

Figure 15. The autocorrelation function computed from the time series of Channel 1 accelerometer data of April 13 is shown in the top panel, plotted in blue. The envelope of the autocorrelation, computed via the discrete Hilbert transform, is shown in the lower panel, in red, on a semi-log scale. The best-fit slope of -0.03295 (for lags τ between 2 and 80 seconds) yields an estimate $\zeta = 0.00420$ (or 0.42%) for the damping coefficient associated with the dominant modal resonance, which is at $\sim$1.25 Hz. The corresponding envelope of the exponential-decay curve is drawn in red in the top plot.

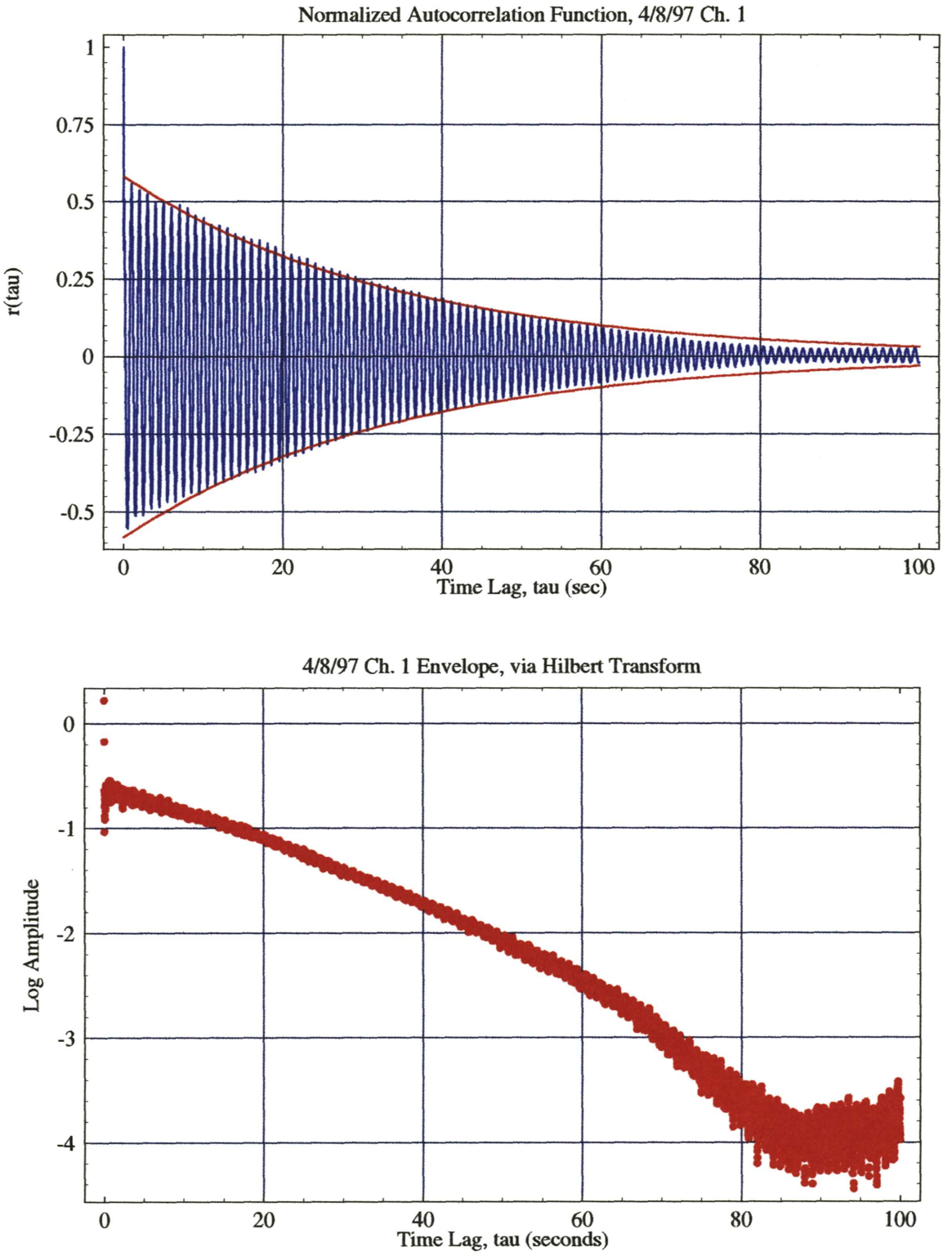

Figure 16. The autocorrelation function computed from the time series of Channel 1 accelerometer data of April 8 is shown in the top panel, and the computed envelope of the autocorrelation in the lower panel. More curvature is evident in this case than in Figure 15. The best-fit slope of -0.0295 (for lags τ between 2 and 50 seconds) yields an estimate $\zeta = 0.0047$ (or 0.47%) for the damping coefficient associated with the dominant modal resonance, which is at $\sim$1 Hz. The corresponding envelope of exponential decay is shown in the top plot.